ACCOUNTS
of chemical research

# A New Class of Semiconducting Polymers for Bulk Heterojunction Solar Cells with Exceptionally High Performance

YONGYE LIANG AND LUPING YU*

*Department of Chemistry and James Franck Institute, The University of Chicago, 929 E 57th Street, Chicago, Illinois 60637*

RECEIVED ON FEBRUARY 18, 2010

## CONSPECTUS

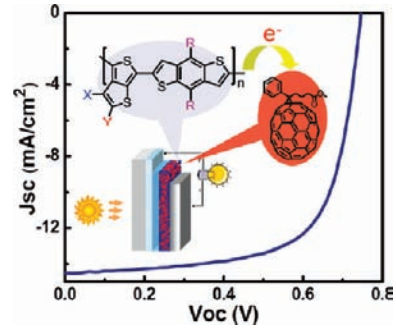


Solar cells based on the polymer–fullerene bulk heterojunction (BHJ) concept are an attractive class of low-cost solar energy harvesting devices. Because the power conversion efficiency (PCE) of these solar cells is still significantly lower than that of their inorganic counterparts, however, materials design and device engineering efforts are directed toward improving their output. A variety of factors limit the performance of BHJ solar cells, but the properties of the materials in the active layer are the primary determinant of their overall efficiency.

The ideal polymer in a BHJ structure should exhibit the following set of physical properties: a broad absorption with high coefficient in the solar spectrum to efficiently harvest solar energy, a bicontinuous network with domain width within twice that of the exciton diffusion length, and high donor–acceptor interfacial area to favor exciton dissociation and efficient transport of separated charges to the respective electrodes. To facilitate exciton dissociation, the lowest unoccupied molecular orbital (LUMO) energy level of the donor must have a proper match with that of the acceptor to provide enough driving force for charge separation. The polymer should have a low-lying highest occupied molecular orbital (HOMO) energy level to provide a large open circuit voltage ($V_{oc}$). All of these desired properties must be synergistically integrated to maximize solar cell performance. However, it is difficult to design a polymer to fulfill all these requirements.

In this Account, we summarize our recent progress in developing a new class of semiconducting polymers, which represents the first polymeric system to generate solar PCE greater than 7%. The polymer system is composed of thieno[3,4-*b*]-thiophene and benzodithiophene alternating units. These polymers have low bandgaps and exhibit efficient absorption throughout the region of greatest photon flux in the solar spectrum (around 700 nm). The stabilization of the quinoidal structure from thieno[3,4-*b*]thiophene is believed to be primarily responsible for these properties. Additionally, the rigid backbone enables the polymer to form an assembly with high hole mobility. Proper side chains on the polymer backbone ensure good solubility and miscibility with fullerene acceptors. The flexibility in structural tuning on the polymer backbone provides the polymers with relatively low-lying HOMO energy levels and enhanced $V_{oc}$, short-circuit current density ($J_{sc}$), and fill factor (FF) and, thus, enhanced PCE.

All of these features indicate that the polymer system exhibits a host of properties that are indeed synergistically combined, leading to the enhancement in solar cell output. Our preliminary results demonstrate why these polymers are excellent materials for solar energy conversion and represent prime candidates for further improvements through research and development.

## 1. Introduction

From the considerations of energy sustainability and environmental protection, solar energy is the largest carbon-neutral energy source to be explored and utilized much more extensively.[1] There are solar cell devices based on inorganic semiconductors currently on the market that already efficiently harvest solar energy. These

Published on the Web 07/13/2010 www.pubs.acs.org/acr
10.1021/ar1000296 

devices are now being installed in solar factories and on rooftops of buildings. However, the cost of these devices is still too high to be economically viable.[2] The urgency of securing sustainable energy resources for the world calls upon the scientific community to develop new materials for the cost-effective harvest of solar energy. This is the major motivation for the development of organic photovoltaic (OPV) materials and devices, which are envisioned to exhibit advantages such as low cost, high device flexibility, and fabrication from highly abundant materials.[3] Although there are skeptics in the solar energy community, the past success in organic light emitting diodes provides scientists with confidence that organic photovoltaic devices will provide vital alternatives to their inorganic counterparts.[4]

There are two general architectures in organic solar cell devices (Figure 1).[5] At the early stage of development, Tang utilized donor−acceptor double layers to introduce a chemical potential at the interface to facilitate charge separation after excitation by incident light.[6] The planar heterojunction offers a simple configuration of organic solar cell devices and has been widely used in small molecule solar cells, especially in those prepared via vapor deposition.[7] PCE around 4% has been achieved in the double layer copper phthalocyanine/$C_{60}$ solar cells.[8] However, it is difficult to further enhance the efficiency in such structures due to their small interfacial areas and the limited thickness required for the short exciton diffusion length.[5] A proposed approach to optimize the donor−acceptor interface and charge transport pathway is to construct a well-ordered heterojunction by incorporating interdigited nanocolumns of both donor and acceptor.[9] This approach has had limited success so far, one of the reasons for which is the lack of an effective approach to assemble materials into desired supramolecular structures with controlled domain orientations.[10]

So far, the most successful architecture to build organic photovoltaic solar cells is the BHJ structure prepared by mixing donors and acceptor with nanoscale phase separation.[11,5] The BHJ structure offers a high density of heterojunction interfaces in the device, and the structure can be easily implemented. In addition, it allows for a quick survey of the best composition of materials in the active layer.[5] The composite active layer can be prepared by solution or vacuum deposition techniques. Solution-processed BHJ solar cells offer the possibility of manufacturing the composite active layer over a large area in one simple step at room temperature, which can be very effective both in cost and in energy.[12]

There are generally two components in the BHJ structure, donor and acceptor. Selection of the materials in both components is very important for the solar cell performance. As donor materials, semiconducting polymers have shown better performance than their small-molecule counterparts due to their ability to more efficiently form films from solution and the higher charge mobility typical of the blend. In the acceptor component, fullerene derivatives are the best candidates so far due to their high electron affinity, superior electron mobility and three-dimensional structure, providing unique packing ability in blend to efficiently form electron transport channels.[13] The original fullerenes do not have enough solubility in organic solvents, so fullerene derivatives with solubilizing groups are usually used, such as [6,6]-phenyl-$C_{61}$-butyric acid methyl ester ($PC_{61}BM$).[14] As a result, the most effective composite structure in solution-processed BHJ organic solar cells is based on a conjugated polymer/fullerene derivative blend.

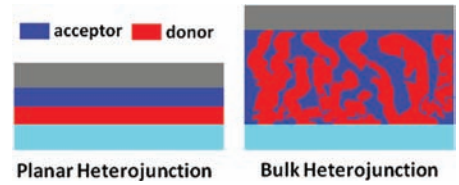


**FIGURE 1.** Architectures of organic solar cells.

Detailed studies by many groups in the past years have brought about steady progress in this field. During this process, poly(3-hexylthiophene) (P3HT) has played a very important role as a donor material.[15] PCE of about 5% has been achieved in solar cells based on P3HT/$PC_{61}BM$ derivatives.[16] The efficiency of polymer solar cells is still significantly lower than that of their inorganic counterparts, such as silicon, CdTe, and copper indium gallium selenide (CIGS), which prevents them from practical implementation on a large scale.[2] New materials exhibiting better performances are needed in order to achieve the desired performance in these types of solar cells for practical application.

The development of new polymers requires careful consideration of several issues including absorption, energy level, hole mobility, and miscibility with fullerenes, which are mentioned above.[17] It is difficult to design a polymer to fulfill all these requirements. Current polymer solar cells often suffer from inferior properties in some or all of these parameters due to a variety of issues related to the nature of the materials and device engineering. So far, besides the P3HT system, there are only a few polymer solar cell systems reported that exceed 5% in power conversion efficiency.[18]

Recently, our group has developed a series of new semiconducting polymers with thieno[3,4-*b*]thiophene and benzodithiophene alternating units. They exhibited superior solar

**SCHEME 1.** Synthetic Schemes for Polymers PTB1−PTB6

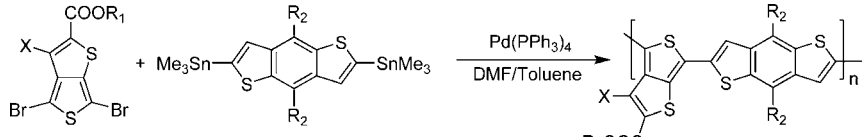


**PTB1**: X = H, $R_1$ = n-dodecyl, $R_2$ = n-octyloxy
**PTB2**: X = H, $R_1$ = 2-ethylhexyl, $R_2$ = n-octyloxy
**PTB3**: X = H, $R_1$ = 2-ethylhexyl, $R_2$ = n-octyl

**PTB4**: X = F, $R_1$ = n-octyl, $R_2$ = 2-ethylhexyloxy
**PTB5**: X = H, $R_1$ = n-octyl, $R_2$ = 2-ethylhexyloxy
**PTB6**: X = H, $R_1$ = 2-butyloctyl, $R_2$ = n-octyloxy

energy PCE to polymers disclosed in the literature in BHJ polymer solar cells in combination with fullerene derivatives as acceptors.[19] Solar power conversion efficiency has reached close to 8%.

## 2. Synthesis of Polymers

The polymers were designed based on the considerations discussed above. Scheme 1 shows the structures and synthetic scheme of the new polymers. The key monomer contains the thieno[3,4-*b*]thiophene moiety that can support the quinoidal structure and lead to a narrow polymer bandgap, which is crucial to efficiently harvest solar energy.[20] In our past efforts, we found that incorporation of this monomer into polymers indeed lowered the band gap of the resulting conjugated polymers. Since the thieno[3,4-*b*]thiophene moiety is very electron-rich, an electron-withdrawing ester group is introduced to stabilize the resulting polymers.[21] The benzo[1,2-*b*:4,5-*b*′]-dithiophene monomers are chosen because of their more extended conjugated systems and proper side chain patterns for enhanced solubility.[22]

The Stille polycondensation between the ester-substituted 2,5-dibromothieno[3,4-*b*]thiophene and benzodithiophene distannane monomers (Scheme 1) led to the synthesis of these polymers in high yield.[19] We have found that the Stille polycondensation is an ideal approach to these functionalized semiconducting polymers because it can tolerate functional groups such as esters and the homogeneous reaction conditions can be beneficial for high polymerization degree.[23] These polymers exhibit relatively high molecular weight and are soluble in halogenated solvents.

The basic electro-optic properties of these polymers are very similar to one another (See Table 1). For example, all of these polymers exhibit identical absorption spectra, with only slight changes in the absorption peak and onset point (Figure 2). The HOMO energy levels of the polymers, as determined by cyclic voltammetry (CV), are very close to one another with the exceptions of those observed for PTB3 and PTB4 (Table 1). From the comparison of PTB2 with PTB3, it is noticed that the HOMO energy level of the polymer is lowered from −4.94 to −5.04 eV by the substitution of an alkoxyl side chain for an alkyl side chain. Comparing PTB4 with PTB5, polymers with the same side chain patterns, shows that the introduction of the electron-withdrawing fluorine in the polymer backbone significantly lowers the HOMO level. It shows that the HOMO energy level of the polymer can be lowered by substituting a less electron-rich group in the side chain (i.e., replacement of alkoxyl with an alkyl side chain) or by introduction of electron-withdrawing groups (i.e., fluorine) to the backbone.

**TABLE 1.** Characteristic Properties of Polymers and Their Solar Cells in PTB*x*/$PC_{61}BM$ Composite

| polymers | $E_{HOMO}$ (eV) | $E_{LUMO}$ (eV) | $V_{oc}$ (V) | $J_{sc}$ (mA/cm$^2$) | FF (%) | PCE (%) |
|---|---|---|---|---|---|---|
| PTB1 | −4.90 | −3.20 | 0.58 | 12.5 | 65.4 | 4.76 |
| PTB2 | −4.94 | −3.22 | 0.60 | 12.8 | 66.3 | 5.10 |
| PTB3 | −5.04 | −3.29 | 0.74 | 13.1 | 56.8 | 5.53 |
| PTB4 | −5.12 | −3.31 | 0.76 | 9.20 | 44.5 | 3.10 |
| PTB5 | −5.01 | −3.24 | 0.68 | 10.3 | 43.1 | 3.02 |
| PTB6 | −5.01 | −3.17 | 0.62 | 7.74 | 47.0 | 2.26 |
| PTB3[a] | | | 0.72 | 13.9 | 58.5 | 5.85 |
| PTB4[a] | | | 0.74 | 13.0 | 61.4 | 5.90 (6.1[b]) |
| PTB5[a] | | | 0.66 | 10.7 | 58.0 | 4.10 |

[a] Devices prepared from mixed solvent dichlorobenzene/diiodooctane (97/3, v/v). [b] PCE value obtained after spectral correction.

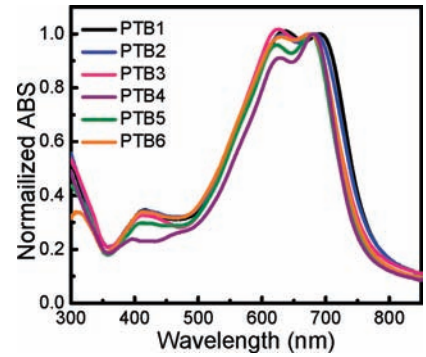


**FIGURE 2.** UV−vis absorption spectra of the polymer films.

The hole mobility of these polymers varies according to structures: $4.7 \times 10^{-4}$, $4.0 \times 10^{-4}$, $7.1 \times 10^{-4}$, $7.7 \times 10^{-4}$, $4.0 \times 10^{-4}$, and $2.6 \times 10^{-4}$ cm$^2$/(V·s) are found for PTB1, PTB2, PTB3, PTB4, PTB5, and PTB6, respectively, from the space charge limited current (SCLC) method.[24] The alkyl-grafted PTB3 and fluorinated PTB4 exhibit larger hole mobilies than those of the other polymers.

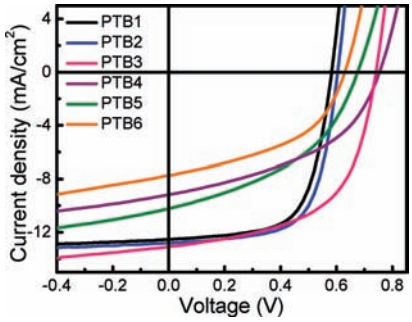


**FIGURE 3.** Current−voltage characteristics of polymer/$PC_{61}BM$ solar cells under AM 1.5 conditions (100 mW/cm$^2$).

## 3. Photovoltaic Effect of PTB*x*/$PC_{61}BM$ Composites

Photovoltaic properties of all of the polymers were investigated in polymer solar cell devices fabricated in structures of ITO/PEDOT:PSS/polymer:$PC_{61}BM$ (1:1, wt ratio)/Ca/Al. Representative characteristics of the solar cells are summarized in Table 1 and Figure 3. The active layer thickness was around 100−110 nm, which was shown to be the optimal thickness for this material system.

The solar cells prepared from PTB1/$PC_{61}BM$ composites showed a short-circuit current, $J_{sc}$, of 12.5 mA/cm$^2$, a $V_{oc}$ of 0.58 V, and a fill factor of 65.4%. The resulting PCE was thus 4.76%. Those from PTB2 showed enhancement from PTB1. The alkyl-substituted PTB3 had an enhanced $V_{oc}$ compared with PTB2. The fluorinated polymer PTB4 devices showed an increase in $V_{oc}$ compared with PTB5. The changes in $V_{oc}$ are well correlated with the HOMO energy levels of the polymers. With the increase of $V_{oc}$, the PTB2 solar cell showed a larger PCE than PTB1. From comparison of PTB2 and PTB3 with similar side chain patterns, PTB3 had a larger $J_{sc}$ than PTB2, which is due to the increase of hole mobility in PTB3. With the increase in $J_{sc}$ and $V_{oc}$, the PTB3 device showed a PCE of 5.53%. However, with the exceptions of PTB2 and PTB3, the other polymer solar cells suffered a significant decrease in $J_{sc}$ and FF compared with the PTB1 solar cell.

The performances of polymers in solar cell devices were found to be related to the morphology of composite films, which has a large effect on a BHJ polymer solar cell.[25] Transmission electron microscopy (TEM) studies revealed fine features in PTB1/$PC_{61}BM$ blend films, indicating continuous interpenetrating networks with small domains. Large domains were observed from $PC_{61}BM$ blend films of PTB5 or PTB6 with more bulky side chains and their solar cell performances were significantly reduced. With the same side chain patterns as PTB5, the fluorinated PTB4 also suffered from suboptimal morphology, and large features (over 100 nm) could be observed in the TEM image of the PTB4/$PC_{61}BM$ blend film (Figure 4). Although PTB4 showed both the lowest HOMO energy level and the largest hole mobility, its photovoltaic performance in simple polymer/$PC_{61}BM$ solar cells was modest (3.10%).

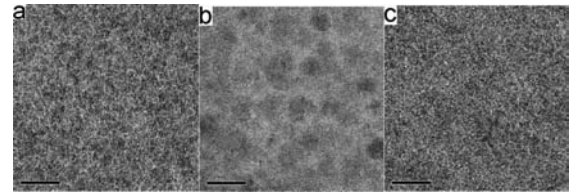


**FIGURE 4.** TEM images of polymer/$PC_{61}BM$ blend films: (a) PTB1, (b) PTB4, and (c) PTB4/$PC_{61}BM$ blend films prepared from mixed solvents dichlorobenzene/diiodooctane (97/3, v/v). The scale bar is 200 nm.

This morphological effect was also demonstrated by studies on thermal annealing of the PTB1/$PC_{61}BM$ blend film. It is known that thermal annealing of P3HT/$PC_{61}BM$ films resulted in increased ordering of the P3HT domains and red-shifted optical absorption features, which produced an enhancement in the PCE in solar cells.[26] Conversely, annealing PTB1/$PC_{61}BM$ film reduced device PCE to 1.92% from 4.76% of the pristine film.[27] The TEM image of pristine film showed very fine, intertwined, fibrous features (i.e., ∼5 nm width), suggesting a better donor−acceptor interaction. The annealed film, however, showed large phase-separated $PC_{61}BM$-enriched domains with sizes ranging from 10 to 200 nm. The larger feature size indicates a smaller surface area to volume ratio of the domains, which reduces the interfacial surface area between polymer and $PC_{61}BM$ and thereby lowers the exciton splitting efficiency. Ultrafast spectroscopic studies indicated that the cation yield of the annealed film characterized by the signal at 2.5 ns time delay was only about 43% of that for the pristine film.

The morphological problem could be remedied via use of a mixed solvent in preparing polymer/fullerene spin-coating solution.[28] The PTB4/$PC_{61}BM$ blend film prepared by using dichlorobenzene/1,8-diiodooctane (97/3, v/v) as the solvent exhibited improved morphology. There are no large features in the TEM images, and the film shows similar morphology to that of PTB1 or PTB2 blend films in their TEM images (Figure 4). Dramatic performance enhancements could be observed both in PTB4 and PTB5 solar cells (Figure 5a). Besides the increase of $V_{oc}$, the PTB4 solar cell showed larger $J_{sc}$ and a slight increase of FF compared with that observed in PTB5, due to the higher hole mobility found in the fluorinated PTB4. The PCE from the PTB4/$PC_{61}BM$ solar cell reached 5.9%. After calibration with the spectral mismatch factor, the efficiency of the PTB4/$PC_{61}BM$ solar cell reached 6.1%. Figure 5b shows

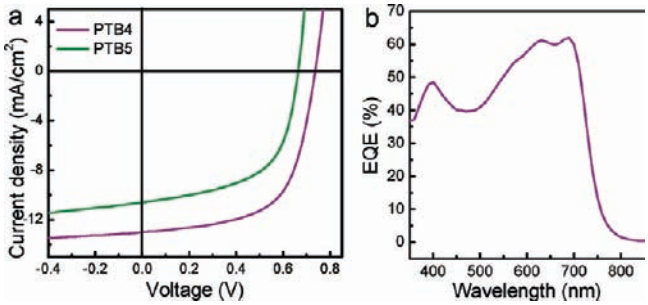


**FIGURE 5.** (a) Current−voltage characteristics of polymer/$PC_{61}BM$ solar cells prepared from mixed solvents dichlorobenzene/diiodooctane (97/3, v/v) under AM 1.5 conditions (100 mW/cm$^2$) and (b) external quantum efficiency of a PTB4/$PC_{61}BM$ device prepared from mixed solvents.

the EQE spectrum of the PTB4/$PC_{61}BM$ solar cell prepared from a mixed solvent system. The device can very efficiently harvest the light in the maximum photon flux region (680 nm), showing over 50% from 550 to 750 nm.

## 4. Photovoltaic Effect of PTB*x*/$PC_{71}BM$ Composites

The PCE of these polymer solar cells can be further enhanced by using $PC_{71}BM$ instead of $PC_{61}BM$. The absorption spectra of the PTB1/$PC_{71}BM$ film exhibited a stronger absorption in the spectral range between 400 and 580 nm than that of the $PC_{61}BM$ composite (Figure 6a).[29] This led to a higher $J_{sc}$ of 15.0 mA/cm$^2$, as indicated by the much higher EQE values. The device exhibited a $V_{oc}$ of 0.56 V and a fill factor of 63.3%, which yielded an impressive PCE of 5.6% after correction of the spectral mismatch factor.

Most recently, we further developed a new polymer from the PTB family, PTB7 (Figure 7 inset), which exhibited an excellent photovoltaic effect (Figure 7).[19c] A power conversion efficiency of about 7.4% has been achieved from PTB7/$PC_{71}BM$ solar cell devices, which is the first polymer solar cell system showing power conversion efficiency over 7%. As shown in the structure of PTB7, it seems that the branched

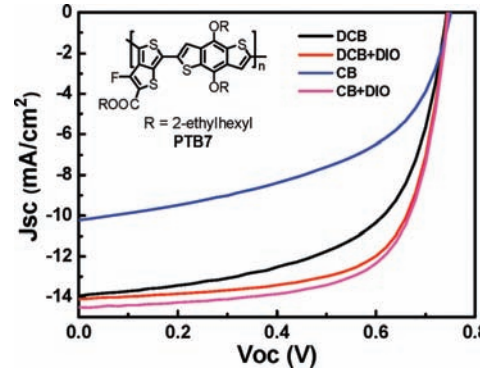


**FIGURE 7.** *J*−*V* curves of PTB7/$PC_{71}BM$ devices using (a) DCB only, (b) DCB with 3% DIO, (c) CB, and (d) CB with 3% DIO as solvents. The structure of PTB7 is shown in inset. Reprinted from reference 19c with permission Copyright Wiley@VCH.

**TABLE 2.** Device Photovoltaic Parameters of DCB Only, DCB with 3% DIO, CB, and CB with 3% DIO as Solvents and $J_{sc}$ Calculated from EQE Spectrum

| | $V_{oc}$ (V) | $J_{sc}$ (mA/cm$^2$) | FF (%) | PCE (%) | $J_{sc}$ (calcd) (mA/cm$^2$) |
|---|---|---|---|---|---|
| DCB | 0.74 | 13.95 | 60.25 | 6.22 | |
| DCB/DIO | 0.74 | 14.09 | 68.85 | 7.18 | 13.99 |
| CB | 0.76 | 10.20 | 50.52 | 3.92 | |
| CB/DIO | 0.74 | 14.50 | 68.97 | 7.40 | 14.16 |

side chains in ester and benzodithiophene render the polymer highly soluble in organic solvents and highly miscible with fullerenes. Although the side chains are branched, the PTB7 has a relatively high hole mobility of approximately 5.8 $\times$ 10$^{-4}$ cm$^2$/(V·s) measured from the SCLC model.

Table 2 shows the comparison of solar cell performances as a function of solvent composition. The best performances of solar cells based on the PTB7/$PC_{71}BM$ blend film were obtained by using a mixed solvent system in preparing the films. Devices prepared from the mixed solvent system consisting of dichlorobenzene (DCB)/1,8-diiodooctane (97%:3% by volume) exhibited a fill factor of 68.9% and a $J_{sc}$ of 14.09 mA. A PCE of 7.18% was obtained. When chlorobezene was used as the cosolvent, the solar cell $J_{sc}$ significantly increased

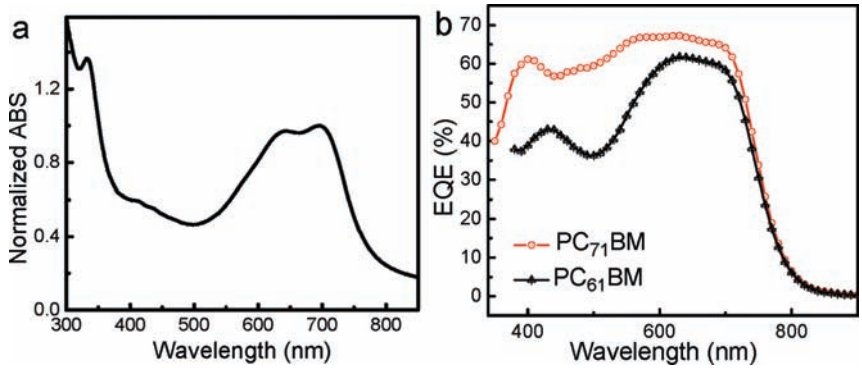


**FIGURE 6.** (a) UV−vis absorption spectrum of PTB1/$PC_{61}BM$ and (b) external quantum efficiency of PTB1/$PC_{61}BM$ and PTB1/$PC_{71}BM$ devices. Reprinted from reference 19c with permission Copyright Wiley@VCH.

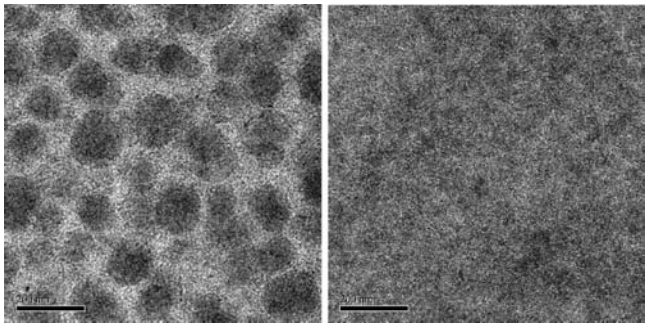

**FIGURE 8.** TEM images of PTB7/$PC_{71}BM$ blend film prepared from chlorobenzene without (left) and with (right) diiodooctane. The scale bar is 200 nm. Reprinted from reference 19c with permission Copyright Wiley@VCH.

to 14.5 mA/cm$^2$ and the fill factor increased to 69%. The combined effect was power conversion efficiency of 7.40%.

Again, the dramatic enhancement of photovoltaic performance is caused by the change in morphology of the blend film. The TEM images (Figure 8) clearly showed that there are large domains (about 100−200 nm in diameter) in the blend film prepared from chlorobenzene, which could diminish exciton migration to the donor−acceptor interface and is not favorable for charge separation. The morphology of the blend film prepared from chlorobenzene/diiodooctane was much more uniform, and there is no large phase separation, showing good miscibility between PTB7 and $PC_{71}BM$ and the formation of interpenetrating networks.

These solar cells exhibited high photoconversion efficiency in the range between 400 and 700 nm with EQE values of over 50% (Figure 9a). A maximum EQE of 68.1% at 630 nm was obtained, which represents one of the highest EQE values in organic solar cells from a low band gap polymer system disclosed in the literature. These measurements are rather accurate as further examined by integrating the EQE data with the AM1.5G solar spectrum. The calculated $J_{sc}$ is 14.2 mA/cm$^2$ in the CB/DIO device. Compared to the experimental $J_{sc}$ of 14.5 mA/cm$^2$, it represents an error of ∼2%. The internal quantum efficiency (IQE) of these cells was estimated based on the following simple facts and assumptions: (a) 4% light loss at air ($n$ = 1)/glass ($n$ = 1.5) interface; (b) metal as perfect mirror (i.e., film absorbs light twice); (c) ignore the absorption in the glass, ITO, and PEDOT:PSS in real device. These solar cells also exhibited a high IQE value over 90% in a wide range of 420 to 660 nm, and the maximum IQE reaches 92%. (Figure 9b) The wide and high IQE data unambiguously proves the very high quality of the new polymer system. In this system, the exciton dissociation, charge transport in donor and acceptor networks, and charge extraction in both organic/electrode interfaces are all very close to 100%. These facts imply that the morphology of blend films is close to an ideal donor and acceptor bicontinuous interpenetrating network in nanoscale.

In collaboration with Solarmer Energy Company, we further modified the polymer structures by using ketone groups to replace the ester groups in polymer PTB4.[30] The resulting polymers exhibited a lower HOMO energy level of 5.22 eV. This slight change did not alter the properties of polymer assembly and charge transport behavior but further increased the $J_{sc}$ to 15.2 mA, resulting in a polymer solar cell with a power conversion efficiency as high as 7.7%.

## 5. Unique Features of These Polymers

Several factors synergistically combine to make these polymers good materials for polymer solar cells exhibiting high power conversion efficiency. First of all, these polymers possess an optimal bandgap of ∼1.6 eV, as well as preferred energy levels that match well with PCBM. As shown in Scheme 1, the flexibility in structural modification makes it possible to fine-tune the energy levels of polymers, which has shown significant effect in enhancing the solar PCE. For example, the introduction of fluorine into the thieno[3,4-*b*]thiophene provides the polymer a relatively low-lying HOMO energy level, which offers enhanced $V_{oc}$.[31] The high PCE is the direct result of the proper match of energy levels.

Second, the thieno[3,4-*b*]thiophene unit can stabilize the quinoidal structure in the polymer chain and thus enhance the planarity along the aromatic polymer backbone. The benzodithiophene unit makes the polymer backbone much more rigid than P3HT. For example, the absorption spectrum of P3HT exhibits a large red shift when the solution spectrum is compared with that of solid state films.[32] This is caused by forced planarity in the solid state due to bond twisting. The PTB*x* series of polymers show minimal shifts in their absorption peaks between solution and solid states. The planarity and conjugation length of the polymer shows little change with the introduction of $PC_{61}BM$, as illustrated by the small change in the absorption of the blend film at longer wavelengths. The rigidity and planarity of the polymer backbone is directly responsible for the high SCLC mobility of the polymers. The high hole mobility and the capability of forming balanced carrier mobility in the blend lead to a high fill factor. The mobility value reported by us based on SCLC is underestimated due to the limitation in our measurement facility. However, under similar conditions, our polymers always exhibit larger charge carrier mobility than the P3HT system.

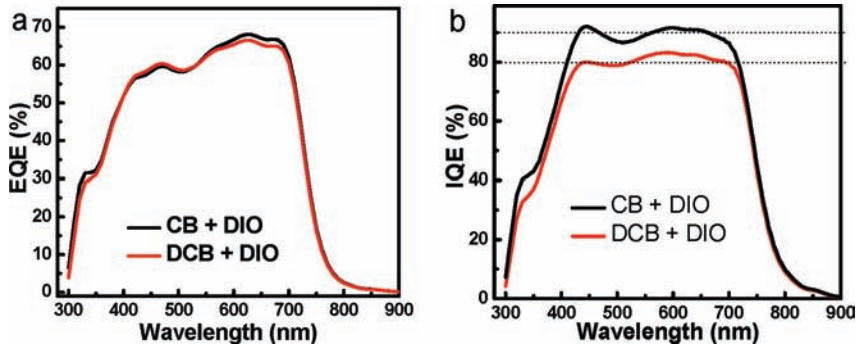


**FIGURE 9.** (a) EQE spectra of champion cells from DCB with 3% DIO and CB with 3% DIO and (b) IQE spectra derived from the EQE and absorption spectra.

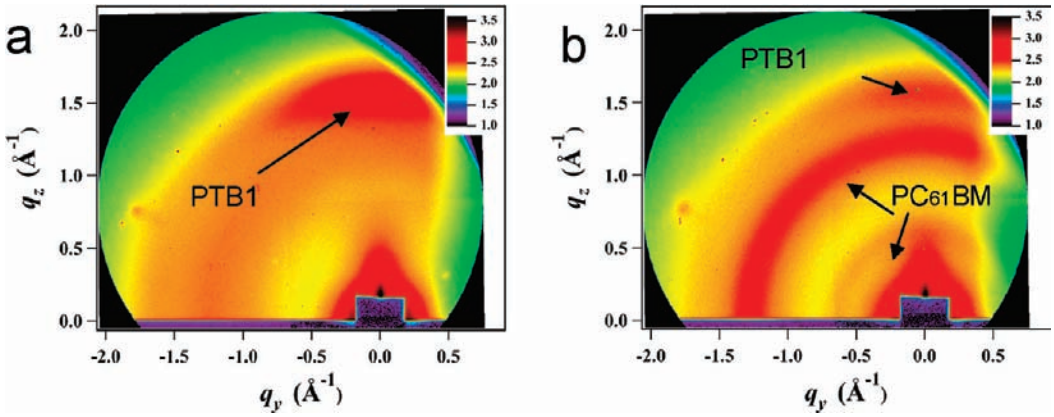


**FIGURE 10.** GISAXS images of (a) polymer PTB1 film and (b) pristine PTB1/$PC_{61}BM$ (1:1) film.

Third, the polymer blend systems have a preferred morphology with interpenetrating networks that can benefit not only the charge separation but also the charge transport, which leads to the high fill factor. Atomic force microscopy (AFM) and TEM studies revealed that the morphology of the PTB1/$PC_{61}BM$ blend film exhibited very fine domains and no large phases can be found (Figure 4a). Other PTB*x* polymers can form similar morphologies from suitable solvent systems. Small nanofibers (about 5 nm width) are observed in the TEM images and are distributed in the entire image field, indicating more effective donor−acceptor interactions. Ultrafast photoluminescence studies revealed that the PTB1/$PC_{61}BM$ blend film exhibited a higher degree of PL quenching due to the photoinduced charge transfer from the polymer to $PC_{61}BM$ than the corresponding P3HT/$PC_{61}BM$ system. All of these results indicated that the polymer and PCBM formed an effective interpenetrating network in the blend film. Our results indicate that control in morphology to form finely mixed composite structures is crucial to obtain high PCE for the solar cell.

The polymer chain was found to be stacked on the substrate in the face-down conformation.[27] This is very different from the polymer alignment in well-studied P3HT solar cell system and favors charge transport. Grazing incidence X-ray scattering (GIXS) revealed a unique lamellae packing structure with both the $\pi$-conjugated backbone and the side chains parallel to the substrate, as identified in PTB1/$PC_{61}BM$ composite.[27] Figure 10 showed GISAXS images of the PTB1 (a) and PTB1/$PC_{61}BM$ (1:1) pristine (b) films. The neat PTB1 film presented two distinctive intermolecular peaks (Figure 10a) with one at $q = 0.226$ Å$^{-1}$ (corresponding to a *d*-spacing of 27.4 Å) and the other at $q = 1.708$ Å$^{-1}$ ($d = 3.68$ Å). The latter was due to the interchain $\pi-\pi$ stacking between polymer backbones. The 27.4 Å feature was preferentially in-plane, whereas that associated with 3.68 Å was vertically out-of-plane. The results suggest that PTB1 molecules assembled and oriented with the aromatic backbones stacked parallel to the substrate surface and with the stack separation of 27.4 Å defined by the side chains extended parallel to the substrate. This unique molecular packing is one of the reasons behind the higher carrier mobility observed on PTB1 than that of P3HT.

Efficient charge separation was observed in ultrafast spectroscopic studies of PTB1 and PTB1/$PC_{61}BM$ (1:1 in weight ratio) films in the NIR spectral region of 850−1700 nm.[27] (Figure 11) A peak centered at 1150 nm appears at 100 ps after the excitation in pure polymer films, which is assigned to the PTB1 cation due to the interchain charge transfer.[33] This

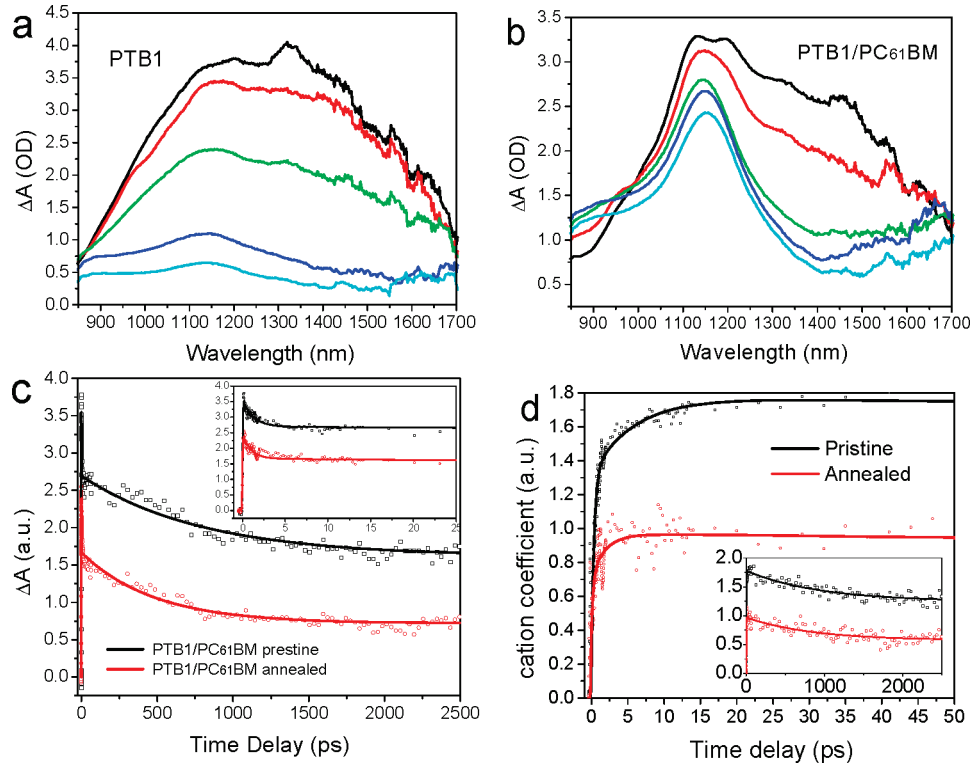


**FIGURE 11.** TA spectra of (a) PTB1 and (b) PTB1/$PC_{61}BM$ (1:1) films in the NIR region with 600 nm excitation wavelength. (c) Kinetic traces of pristine and annealed PTB1/$PC_{61}BM$ films monitored at 1150 nm. The traces are normalized by the number of photons absorbed at 600 nm. The inset shows the same kinetic traces at early delay time. (d) Fitting coefficient of PTB1 cation at different time delay for PTB1/$PC_{61}BM$ pristine and annealed PTB1/$PC_{61}BM$ 1:1 film by using equation: $S(\lambda, t) = N_{ES}(t)A_{ES}(\lambda) + N_{CS}(t)[A_c(\lambda) + A_a(\lambda)] + N_{CT}(t)A_{CT}(\lambda)$.

assignment of the 1150 nm peak to the PTB1 cation is supported by the optical absorption spectra of the same film undergoing electro-spectrochemical oxidation. This 1150 nm peak had a lifetime much longer than a few nanoseconds, suggesting the formation of a new cationic species in the composite film. An increased absorption with time was also observed for the feature above 1500 nm, which could be assigned to free carrier absorption.[34] The appearance of the free PTB1 cation after CS is also consistent with the fluorescence quenching mentioned above.[19a]

It was found that the average CS rate for the pristine PTB1/$PC_{61}BM$ film was 1.5 ps, which is more than twice as fast as the 4 ps observed for the annealed P3HT/$PC_{61}BM$ film.[35] This faster CS rate, combined with higher charge carrier mobility, contributes to the high device efficiency of the PTB1/$PC_{61}BM$ solar cell in addition to more effective light harvesting in the NIR region.

## 6. Conclusions and Outlook

We have developed a semiconducting polymer system that exhibited excellent solar cell power conversion efficiencies close to 8%. This high solar cell performance originates from synergistic combinations of desired properties in a single polymer system. Detailed structural fine-tuning is the key to modify the properties of semiconducting polymers. The system discussed here is a promising platform for further development of new and better polymeric photovoltaic materials with high PCE.

Stability is another important issue to be addressed before the widespread use of polymer solar cells.[3] Generally, careful device engineering, like cell encapsulation to protect the active materials from oxygen and moisture, plays an important role to increase the stability and durability of solar cell devices. More importantly, the polymer material must have suitable photochemical stability, which can be achieved by careful design of and tuning in polymer structures. Careful selection of the side chain patterns could increase the miscibility with fullerene compounds and enhance the morphological stability of BHJ structures. Perhaps, one should consider use of thermally or photochemically cross-linkable moieties to enhance the structural stability of the polymer and composite. Stability of solar cells from thieno[3,4-*b*]-thiophene−benzodithiophene-based polymers is currently under study. Preliminary results suggest that these polymer solar cells are stable under illumination for over 2400 h in a glovebox. The lifetime of polymer solar cells has been projected to be over 20 000 h in low-efficiency devices.[36] It is believed that further work on optimization of polymer struc-

tures and device engineering will lead to materials stable enough for commercialization. Close collaboration among scientists in different disciplines will be the key to future advances in this exciting area.

Our results point to a bright future in polymer solar cell research. We can safely predict that polymeric solar cells will be successful.

*We would like to acknowledge support from NSF, AFOSR, DOE, NSF-MRSEC, and Solarmer Energy Inc. for the works described here. We thank Professor Lin Chen (Argonne National Labs and Northwestern University), Drs. Gang Li and Yue Wu (Solarmer Energy Inc.) for their help in characterizing these materials. Students and postdoctoral associates whose names are shown in the cited papers are also acknowledged.*

## BIOGRAPHICAL INFORMATION

**Yongye Liang** was born in Guangdong Province, People's Republic of China. He received his B.S. degree in chemistry from Nanjing University in 2003. He then completed his Ph.D. degree in 2009 from Department of Chemistry at the University of Chicago, under the guidance of Professor Luping Yu. Currently, he is a postdoctoral associate at Stanford University.

**Luping Yu** was born in Zhejiang Province, People's Republic of China. He received his B.S. (1982) and M.S. (1984) degrees in polymer chemistry from Zhejiang University and his Ph.D. degree (1989) from The University of Southern California. He is currently a Professor of Chemistry at the University of Chicago. His current research focuses on polymer chemistry, surface chemistry, and supramolecular chemistry. Typical examples of current projects include (1) conjugated diblock copolymers for the formation of self-assembled, nanosized electroactive materials, (2) molecular electronics, (3) photoinduced electron transfer and photovoltaic materials, (4) gene transfer polymers, and (5) nanoporous hydrogen storage polymeric materials.

## REFERENCES

1 Lewis, N. S. *Global Energy Prospective. Solar Energy Workshop*; US Department of Energy: Washington, DC, 2005.

2 (a) Hsieh, J. S. *Electric Power Generation. Solar Energy Engineering*; Prentice-Hall: NJ, 1986. (b) Green, M. A.; Emery, K.; King, D. L.; Igari, S.; Warta, W. Solar Cell Efficiency Tables (Version 18). *Prog. Photovoltaics* **2001**, *9*, 287–293.

3 Brabec, C. J. Organic Photovoltaics: Technology and Market. *Sol. Energy Mater. Sol. Cells* **2004**, *83*, 273–292.

4 (a) D'Andrade, B. W.; Forrest, S. R. White Organic Light-emitting Devices for Solid-state Lighting. *Adv. Mater.* **2004**, *16*, 1585–1595. (b) Reineke, S.; Lindner, f.; Schwartz, G.; Seidler, N.; walzer, K.; Lussem, B.; Leo, K. White Organic Light-emitting Diodes with Fluorescent Tube Efficiency. *Nature* **2009**, *459*, 234–238. (c) Wu, H. B.; Ying, L.; Yang, W.; Cao, Y. Progress and Perspective of Polymer White Light-emitting Devices and Materials. *Chem. Soc. Rev.* **2009**, *38*, 3391–3400.

5 Gunes, S.; Neugebauer, H.; Sariciftci, N. S. Conjugated Polymer-Based Organic Solar Cells. *Chem. Rev.* **2007**, *107*, 1324–1338.

6 Tang, C. W. Two-layer Organic Photovoltaic Cell. *Appl. Phys. Lett.* **1986**, *48*, 183–185.

7 Riede, M.; Mueller, T.; Tress, W.; Schueppel, R.; Leo, K. Small-molecule Solar Cells-Status and Perspectives. *Nanotechnology* **2008**, *19*, 424001.

8 Xue, J. G.; Uchida, S.; Rand, B. P.; Forrest, S. R. 4.2% Efficient Organic Photovoltaic Cells with Low Series Resistances. *Appl. Phys. Lett.* **2004**, *84*, 3013–3015.

9 Coakley, K. M.; McGehee, M. D. Conjugated Polymer Photovoltaic Cells. *Chem. Mater.* **2004**, *16*, 4533–4542.

10 Guo, J.; Liang, Y. Y.; Xiao, S. Q.; Szarko, J. M.; Sprung, M.; Mukhopadhyay, M. K.; Wang, J.; Yu, L. P.; Chen, L. X. Structure and Dynamics Correlations of Photoinduced Charge Separation in Rigid Conjugated Linear Donor-Acceptor Dyads Towards Photovoltaic Applications. *New J. Chem.* **2009**, *33*, 1497–1507.

11 Yu, G.; Gao, J.; Hummelen, J. C.; Wudl, F.; Heeger, A. J. Polymer Photovoltaic Cells: Enhanced Efficiencies via a Network of Internal Donor-Acceptor Heterojunctions. *Science* **1995**, *270*, 1789–1791.

12 Brabec, C. J.; Sariciftci, N. S.; Hummelen, J. C. Plastic Solar Cells. *Adv. Funct. Mater.* **2001**, *11*, 15–26.

13 Brunetti, F. G.; Kumar, R.; Wudl, F. Organic Electronics from Perylene to Organic Photovoltaics: Painting a Brief History with a Broad Brush. *J. Mater. Chem.* **2010**, *20*, 2934–2948.

14 Hummelen, J. C.; Knight, B. W.; LePeq, F.; Wudl, F.; Yao, J.; Wilkins, C. L. Preparation and Characterization of Fulleroid and Methanofullerene Derivatives. *J. Org. Chem.* **1995**, *60*, 532–538.

15 Dennler, G.; Scharber, M. C.; Brabec, C. J. Polymer-Fullerene Bulk-heterojunction Solar Cells. *Adv. Mater.* **2009**, *21*, 1323–1338.

16 (a) Li, G.; Shrotriya, V.; Yao, Y.; Yang, Y. Investigation of Annealing Effects and Film Thickness Dependence of Polymer Solar Cells Based on Poly(3-hexylthiophene). *J. Appl. Phys.* **2005**, *98*, 043704. (b) Ma, W. L.; Yang, C. Y.; Gong, X.; Lee, K. H.; Heeger, A. J. Thermally Stable, Efficient Polymer Solar Cells with Nanoscale Control of the Interpenetrating Network Morphology. *Adv. Funct. Mater.* **2005**, *15*, 1617–1622. (c) Reyes, R. M.; Kim, K.; Carroll, D. L. High-efficiency Photovoltaic Devices Based on Annealed Poly(3-hexylthiophene) and 1-(3-methoxycarbonyl)-propyl-1-phenyl-(6,6)C-61 Blends. *Appl. Phys. Lett.* **2005**, *87*, 083506. (d) Kim, J. Y.; Kim, S. H.; Lee, H. H.; Lee, K.; Ma, W.; Gong, X.; Heeger, A. J. New Architecture for High-efficiency Polymer Photovoltaic Cells Using Solution-based Titanium Oxide as an Optical Spacer. *Adv. Mater.* **2006**, *18*, 572–576. (e) Irwin, M. D.; Buchholz, D. B.; Hains, A. W.; Chang, R. P. H.; Marks, T. J. p-Type Semiconducting Nickel Oxide as an Efficiency-enhancing Anode Interfacial Layer in Polymer Bulk-hetero Junction Solar Cells. *Proc. Natl. Acad. Sci. U.S.A.* **2008**, *105*, 2783–2787.

17 Roncali, J. Molecular Engineering of the Band Gap of pi-Conjugated Systems: Facing Technological Applications. *Macromol. Rapid Commun.* **2007**, *28*, 1761–1775.

18 (a) Park, S. H.; Roy, A.; Beaupre, S.; Cho, S.; Coates, N.; Moon, J. S.; Moses, D.; Leclerc, M.; Lee, K.-H.; Heeger, A. J. Bulk Heterojunction Solar Cells with Internal Quantum Efficiency Approaching 100%. *Nat. Photonics* **2009**, *3*, 297–302. (b) Peet, J.; Kim, J. Y.; Coates, N. E.; Ma, W. L.; Moses, D.; Heeger, A. J.; Bazan, G. C. Efficiency Enhancement in Low-bandgap Polymer Solar Cells by Processing with Alkane Dithiols. *Nat. Mater.* **2007**, *6*, 497–500.

19 (a) Liang, Y. Y.; Wu, Y.; Feng, D. Q.; Tsai, S.-T.; Li, G.; Son, H. J.; Yu, L. P. Development of New Semiconducting Polymers for High Performance Solar Cells. *J. Am. Chem. Soc.* **2009**, *131*, 56–57. (b) Liang, Y. Y.; Feng, D. Q.; Wu, Y.; Tsai, S.-T.; Li, G.; Ray, C.; Yu, L. P. Highly Efficient Solar Cell Polymers Developed via Fine-tuning Structural and Electronic Properties. *J. Am. Chem. Soc.* **2009**, *131*, 7792–7799. (c) Liang, Y. Y.; Xu, Z.; Xia, J. B.; Tsai, S. T.; Wu, Y.; Li, G.; Ray, C.; Yu, L. P. For the Bright Future- Bulk Heterojunction Polymer Solar Cells with Power Conversion Efficiency of 7.4%. *Adv. Mater.* **2010**, *22*, E135—E138.

20 (a) Wudl, F.; Kobayashi, M.; Heeger, A. J. Poly(isothianaphthene). *J. Org. Chem.* **1984**, *49*, 3382–3384. (b) Pomerantz, M.; Gu, X. M. Poly(2-decylthieno[3,4-b]thiophene). A New Soluble Low-bandgap Conducting Polymer. *Synth. Met.* **1997**, *84*, 243–244. (c) Lee, K. H.; Sotzing, G. A. Poly(thieno[3,4-b]thiophene). A New Stable Low Band Gap Conducting Polymer. *Macromolecules* **2001**, *34*, 5746–5747.

21 (a) Yao, Y.; Liang, Y. Y.; Shrotriya, V.; Xiao, S. Q.; Yu, L. P.; Yang, Y. Plastic Near-infrared Photodetectors Utilizing Low Band Gap Polymer. *Adv. Mater.* **2007**, *19*, 3979–3983. (b) Liang, Y. Y.; Xiao, S. Q.; Feng, D. Q.; Yu, L. P. Control in Energy Levels of Conjugated Polymers for Photovoltaic Application. *J. Phys. Chem. C* **2008**, *112*, 7866–7871. (c) Liang, Y. Y.; Feng, D. Q.; Guo., J. C.; Szarko, J. M.; Claire, R.; Chen, L. X.; Yu, L. P. Regioregular Oligomer and Polymer Containing Thieno-[3,4-*b*]thiophene Moiety for Efficient Organic Solar Cells. *Macromolecules* **2009**, *42*, 1091–1098.

22 Pan, H. L.; Li, Y. N.; Wu, Y. L.; Liu, P.; Ong, B. S.; Zhu, S. P.; Xu, G. Low-Temperature, Solution-Processed, High-Mobility Polymer Semiconductors for Thin-Film Transistors. *J. Am. Chem. Soc.* **2007**, *129*, 4112–4113.

23 Bao, Z. N.; Chan, W. K.; Yu, L. P. Synthesis of Conjugated Polymer by the Stille Coupling Reaction. *Chem. Mater.* **1993**, *5*, 2–3.

24 (a) Malliaras, G. G.; Salem, J. R.; Brock, P. J.; Scott, C. Electrical Characteristics and Efficiency of Single-layer Organic Light-emitting Diodes. *Phys. Rev. B* **1998**, *58*, 13411–13414. (b) Goh, C.; Kline, R. J.; McGehee, M. D.; Kadnikova, E. N.; Frechet, J. M. J. Molecular-weight-dependent Mobilities in Regioregular Poly(3-hexyl-thiophene) Diodes. *Appl. Phys. Lett.* **2005**, *86*, 122110.

25 Yang, X. N.; Loos, J. Toward High-Performance Polymer Solar Cells: The Importance of Morphology Control. *Macromolecules* **2007**, *40*, 1353–1362.

26 (a) Padinger, F.; Rittberger, R.; Sariciftci, N. S. Effects of Postproduction Treatment on Plastic Solar Cells. *Adv. Funct. Mater.* **2003**, *13*, 85–88. (b) Yang, X.; Loos, J.; Veenstra, S. c.; Verhees, W. J. H.; Wienk, M. M.; Kroon, J. M.; Michels, M. A. J.; Janssen, R. A. J. Nanoscale Morphology of High-Performance Polymer Solar Cells. *Nano Lett.* **2005**, *5*, 579–583.

27 Guo, J. C.; Liang, Y. Y.; Szarko, J. M.; Lee, B. D.; Son, H. H.; Rolczynski, B.; Yu, L. P.; Chen, L. X. Structure, Dynamics and Power Conversion Efficiency Correlations in a New Low Bandgap Polymer:PCBM Solar Cell. *J. Phys. Chem. B* **2010**, *114*, 742–748.

28 Lee, J. K.; Ma, W. L.; Brabec, C. J.; Yuen, J.; Moon, J. S.; Kim, J. Y.; Lee, K.; Bazan, G. C.; Heeger, A. J. Processing Additives for Improved Efficiency from Bulk Heterojunction Solar Cells. *J. Am. Chem. Soc.* **2008**, *130*, 3619–3623.

29 Wienk, M. M.; Kroon, J. M.; Verhees, W. J. H.; Knol, J.; Hummelen, J. C.; van Hal, P. A.; Janssen, R. A. J. Efficient Methano[70]fullerene/MDMO-PPV Bulk Heterojunction Photovoltaic Cells. *Angew. Chem., Int. Ed.* **2003**, *42*, 3371–3375.

30 Chen, H. Y.; Hou, J. H.; Zhang, S. Q.; Liang, Y. Y.; Yang, G. W.; Yang, Y.; Yu, L. P.; Wu, Y.; Li, G. Polymer Solar Cells with Enhanced Open-Circuit Voltage and Efficiency. *Nat. Photonics* **2009**, *3*, 649–653.

31 Scharber, M.; Muhlbacher, D.; Koppe, M.; Denk, P.; Waldauf, C.; Heeger A. J.; Brabec, C. Design Rules for Donors in Bulk-Heterojunction Solar Cells - Towards 10% Energy Conversion Efficiency. *Adv. Mater.* **2006**, *18*, 789–794.

32 Li, G.; Yao, Y.; Yang, H. C.; Shrotriya, V.; Yang, G. W.; Yang, Y. Solvent Annealing Effect in Polymer Solar Cells Based on Poly(3-hexylthiophene) and Methanofullerenes. *Adv. Funct. Mater.* **2007**, *17*, 1636–1644.

33 (a) An, Z.; Wu, C. Q.; Sun, X. Dynamics of Photogenerated Polarons in Conjugated Polymers. *Phys. Rev. Lett.* **2004**, *93*, 216407. (b) Miranda, P. B.; Moses, D.; Heeger, A. J. Ultrafast Photogeneration of Charged Polarons in Conjugated Polymers. *Phys. Rev. B* **2001**, *64*, 081201.

34 Guo, J.; She, C.; Lian, T. Ultrafast Electron Transfer between Molecule Adsorbate and Antimony Doped Tin Oxide (ATO) Nanoparticles. *J. Phys. Chem. B* **2005**, *109*, 7095–7102.

35 Hwang, I.-W.; Moses, D.; Heeger, A. J. Photoinduced Carrier Generation in P3HT/PCBM Bulk Heterojunction Materials. *J. Phys. Chem. C* **2008**, *112*, 4350–4354.

36 Krebs, F. C.; Spanggaard, H. Significant Improvement of Polymer Solar Cell Stability. *Chem. Mater.* **2005**, *17*, 5235–5237.